ISSN 1070-3284, Russian Journal of Coordination Chemistry, 2024, Vol. 50, No. 2, pp. 85–95. © Pleiades Publishing, Ltd., 2024.

3D Coordination Polymers with N-Heterocyclic Ga(I) Moieties

T. S. Koptseva[a], E. V. Baranov[a], and I. L. Fedushkin[a, *]

[a] *Razuvaev Institute of Organometallic Chemistry, Russian Academy of Sciences, Nizhny Novgorod, Russia*

**e-mail: igorfed@iomc.ras.ru*

Received July 4, 2023; revised July 27, 2023; accepted July 28, 2023

Abstract—The reactions of bimetallic acenaphthene-1,2-diimine complex $[(Dpp\text{-}bian\text{-}GaCr(CO)_5]_2\text{-}[Na(Thf)_2]_2$ (**I**) (Dpp-bian = 1,2-bis[(2,6-diisopropylphenyl)imino]acenaphthene) with 4,4'-bipyridine (4,4'-Bipy) and 1,3-bis(4-pyridyl)propane (Bpp) in THF gave 3D coordination polymers $[\{(Dpp\text{-}bian)GaCr(CO)_5\}\{Na(4,4'\text{-}Bipy)_3\}]_n$ (**II**) and $[(Dpp\text{-}bian)GaCr(CO)_4Na(Et_2O)(Bpp)_{1,5}]_n$ (**III**), respectively. Compounds **II** and **III** were characterized by elemental analysis and NMR and IR spectroscopy. The molecular structure of **II** was established by X-ray diffraction (CCDC no. 2278024).

Keywords: gallium, chromium, coordination polymers, redox-active ligands

DOI: 10.1134/S1070328423601127

INTRODUCTION

Low valence *p*-element compounds form an important area of modern organometallic chemistry. Their reactivity is similar to that of late transition metal compounds, which makes them suitable catalysts for a variety of reactions [1–3]. Usually, stabilization of the low-valence state of an element is achieved by using bulky ligands. In particular, for gallium atoms, this may be β-diketiminate [4], guanidinate [5–7], and diazadiene [8–11] ligands. To date, the chemistry of derivatives containing a free Ga(I) center has been studied quite extensively [3] and includes various types of reactivity such as oxidative addition [12–14], multiple bond cleavage [15], successive oxidation and C–H bond cleavage [16], and many other reactions. Gallaimidazoles [LGa:] are also versatile ligands in the coordination chemistry of transition metals, acting, most often, as Lewis bases [17–19]. However, the chemistry of compounds combining transition and main group metals is studied less extensively [20]. We prepared complexes of some transition metals containing both neutral and anionic acenaphthenediimine gallaimidazole ligands [(Dpp-bian)Ga:] [21–23]. Study of the reactivity of some of them showed that the reactions preferentially take place at the gallylene moiety, in some cases, involving both the metal and the acenaphthenediimine ligand [24], which is similar to the reactions of digallium compound [(Dpp-bian)Ga–Ga(Dpp-bian)], which we studied in detail earlier [25]. Previously, the bimetallic derivatives [(Dpp-bian)M–M(Dpp-bian)] (M = Al, Ga), which possess a versatile reactivity [25–29], stimulated us to synthesize coordination polymers possessing similar unusual properties. For example, we prepared 1D chains [(Dpp-bian)Ga-Ga(Dpp-bian)(μ2-Bpp)]n [30] and [(Dpp-bian)Ga–Zn(Dpp-bian)(μ2-Dpp)]n [31]. However, the fully occupied coordination sphere of the metal in these compounds precludes cycloaddition reactions, as only one reaction center, namely the metal–metal bond, is present. In continuation of our studies on the synthesis of metal-organic coordination polymers (MOCPs) containing a highly reactive low-valence Ga(I) center, we used the complex $[(Dpp\text{-}bian)GaCr(CO)_5]_2\text{-}[Na(Thf)_2]_2$ (I). We carried out reactions of compound I with 4,4'-bipyridine (4,4'-Bipy) and 1,3-bis(4-pyridyl)propane (Bpp). The products of these reactions are discussed in this paper.

EXPERIMENTAL

Compounds **I**–**III** are sensitive to oxygen and moisture; therefore, all operations on their synthesis, isolation, and identification were performed in vacuum using the Schlenk techniques or under nitrogen atmosphere (Glovebox M. Braun). Toluene, tetrahydrofuran, and diethyl ether were dried over sodium/benzophenone and condensed under vacuum in the flasks just prior to use. thf-d8 was dried over sodium/benzophenone at ambient temperature and condensed under vacuum into the NMR tubes that contained the sample. The compound $[(Dpp\text{-}bian)GaCr(CO)_5]_2[Na(Thf)_2]_2$ [22] was prepared by a known procedure.

IR spectra were obtained on an FSM-1201 instrument in the 3998–449 cm^{-1} range (mineral oil mulls). The ^1H NMR spectra were measured on a Bruker Avance III spectrometer (400 MHz). Elemental analysis was performed on a Vario EL Cube automatic analyzer, thermogravimetric analysis was carried out

on a METTLER TOLEDO TGA/DSC 3+ instrument at 40–500°C in a nitrogen flow at a flow rate of 50 mL per minute and a heating rate of 5 K per minute.

Synthesis of [{(Dpp-bian)GaCr(CO)$_5$}{Na(4,4'-Bipy)$_3$}]$_n$ (II). 4,4'-Bipyridine (0.12 g, 0.8 mmol) was added to a solution of compound **I** (0.25 g, 0.13 mmol) in THF (5 mL). The mixture was heated for 20 min at 80°C. After cooling to room temperature, THF was removed from the reaction mixture almost completely, and toluene was added to obtain a 1 : 5 solvent mixture. The sealed tube was kept for 12 h at 25°C. The precipitated green crystals were separated from the solution by decantation, washed with cold toluene, and dried in vacuo. The yield of **II** was 0.21 g (62%).

^{1}H NMR (400 MHz; C_4D_8O; 298 K; δ, ppm; *J*, Hz): 8.69 (d, 12H, *J* = 6.3, Bipy), 7.67 (d, 12H, *J* = 6.0, Bipy), 7.23–7.18 (m, 2H, toluene), 7.17–7.11 (m, 6H, Ar), 7.11–7.06 (m, 3H, toluene), 6.84 (d, 2H, *J* = 7.0, Ar), 6.70 (d, 1H, *J* = 7.0, Ar), 6.68 (d, 1H, *J* = 7.0, Ar), 5.46 (d, 2H, *J* = 6.8, Ar), 3.84 (sept., 4H, *J* = 6.8, CH-*i*-Pr), 3.64 (m, 2H, THF), 2.32 (s, 3H, toluene), 1.79 (m, 6H, 2H, THF), 1.32 (d, 12H, *J* = 7.0, CH_3-*i*-Pr), 1.07 (d, 12H, *J* = 7.0, CH_3-*i*-Pr).

IR (ν, cm^{-1}): 2020 s, 1933 s, 1893 s, 1614 w, 1597 s, 1522 w, 1513 m, 1487 w, 1434 m, 1407 m, 1354 s, 1318 w, 1256 m, 1216 s, 1179 m, 1139 w, 1109 w, 1067 m, 1043 w, 995 s, 962 w, 928 s, 900 s, 849 m, 808 s, 762 s, 730 m, 680 s, 666 s, 646 w, 623 w, 612 s, 571 m, 504 m, 491 w.

For $C_{76.50}H_{72}N_8O_{5.50}NaCrGa$			
Anal. calcd., %	C, 68.50	H, 5.38	N, 8.30
Found, %	C, 68.48	H, 5.35	N, 8.30

Synthesis of [(Dpp-bian)GaCr(CO)$_4$Na(Et$_2$O)-(Bpp)$_{1,5}$]$_n$ (III). 1,3-Bis(4-pyridyl)propane (0.07 g, 0.4 mmol) was added to a solution of compound **I** (0.25 g, 0.13 mmol) in THF (5 mL). The mixture was heated for 20 min at 80°C. After cooling to room temperature, THF was removed from the reaction mixture almost completely, and diethyl ether was added to obtain a 1 : 5 solvent mixture. The sealed tube was heated for 2 h at 80°C. The precipitated green crystals were separated from the solution by decantation, washed with cold diethyl ether, and dried in vacuo. The yield of **III** was 0.17 g (61%).

^{1}H NMR (400 MHz; C_4D_8O; 298 K; δ, ppm; *J*, Hz): 8.44 (d, 12H, *J* = 6.0, Bpp), 7.17–7.06 (m, 24H, Bpp + Ar), 6.83 (d, 4H, *J* = 7.0, Ar), 6.69 (d, 2H, *J* = 6.8, Ar), 6.67 (d, 2H, *J* = 7.0, Ar), 5.75 (d, 4H, *J* = 6.8, Ar), 3.83 (sept., 8H, *J* = 6.8, CH-*i*-Pr), 3.40 (quart., 8H, *J* = 7.0, Et_2O), 2.66 (t, 8H, *J* = 7.5, Bpp), 1.99 (p, 6H, *J* = 7.7, Bpp), 1.31 (d, 24H, *J* = 7.0, CH_3-*i*-Pr), 1.13 (t, 13H, *J* = 6.8, Et_2O), 1.07 (d, 24H, *J* = 7.0, CH_3-*i*-Pr).

IR (ν, cm^{-1}): 2022 s, 1897 s, 1607 m, 1559 w, 1507 w, 1434 w, 1351 m, 1322 w, 1255 w, 1220 w, 1177 w, 1096 m, 1071 w, 1058 w, 1001 m, 927 m, 897 m, 837 w, 806 s, 763 s, 681 s, 668 s, 620 w, 607 w, 605 w, 568 w, 509 m, 494 w.

For $C_{127}H_{143}N_{10}O_{10}Na_2Cr_2Ga_2$			
Anal. calcd., %	C, 67.52	H, 6.38	N, 6.20
Found, %	C, 67.49	H, 6.34	N, 6.19

X-ray diffraction study of II was carried out on an Agilent Xcalibur E (ω-scan mode, MoK_α-radiation, λ = 0.71073 Å, *T* = 100(2) K) single crystal automated diffractometer. X-ray diffraction data collection, initial reflection indexing, refinement of unit cell parameters, and integration of reflections were carried out using the CrysAlisPro program [32]. The structures were solved by direct methods using the dual-space algorithm in the SHELXT program [33] and refined by the full-matrix least squares method on F^2_{hkl} with the SHELXTL program package [34, 35] in the anisotropic approximation for non-hydrogen atoms. The hydrogen atoms were placed in the geometrically calculated positions and refined isotropically in the riding model with fixed thermal parameters (U_{iso}(H) = 1.5U_{equiv}(C) for CH_3 groups and U_{iso}(H) = 1.2U_{equiv}(C) for other groups). The empirical absorption corrections were applied using the SCALE3 ABSPACK algorithm [36]. In the crystal of **II**, toluene solvation molecules and THF solvation molecules disordered over two sites were found in the general positions, with the occupancy ratio being 0.5 : 0.5 : 1 relative to the {(Dpp-bian)GaCr(CO)$_5$}{Na(4,4'-Bipy)$_3$} complex. The topological analysis of coordination polymer structures was performed with the help of the website topcryst.com [37]. Crystallographic data and X-ray diffraction experiment details for **II** are summarized in Table 1; selected bond lengths and bond angles are given in Table 2.

The crystal structure of **II** is deposited with the Cambridge Crystallographic Data Centre (CCDC no. 2278024; https://www.ccdc.cam.ac.uk/structures/).

RESULTS AND DISCUSSION

The reaction of complex [(Dpp-bian)GaCr-(CO)$_5$]$_2$[Na(Thf)$_2$]$_2$ (**I**) with six molar equivalents of 4,4'-bipyridine in THF affords three-dimensional coordination polymer [{(Dpp-bian)GaCr(CO)$_5$}-{Na(4,4'-Bipy)$_3$}]$_n$ (**II**) (Scheme 1). The reaction product was isolated from a THF–toluene solvent mixture in 62% yield as green crystals. The 3D chain of **II** is formed via coordination of neutral Bipy molecules by sodium cations, with the free {(Dpp-bian)GaCr(CO)$_5$} anions being located in the MOCP cavities.

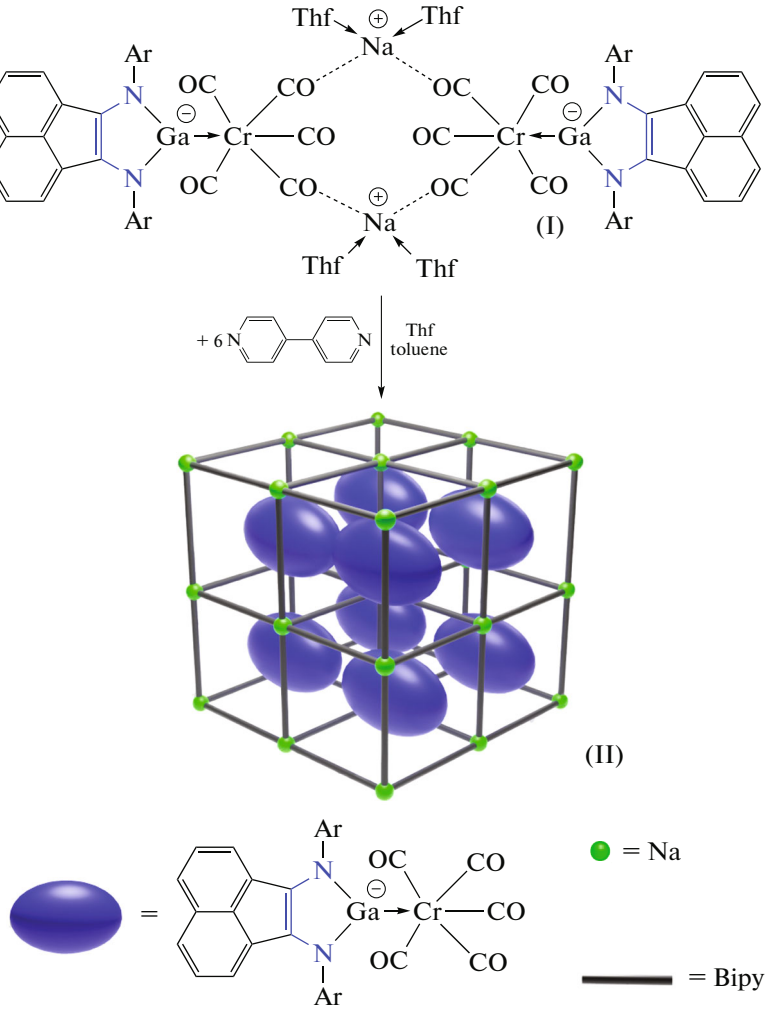

Scheme 1.

The IR spectrum of compound **II** exhibits intense absorption bands at 1893, 1933, and 2020 cm^{-1} frequencies, characteristic of the C–O stretching modes in metal carbonyls. In solution, product **II** apparently dissociates into monomeric species, thus permitting recording of the ^1H NMR spectrum (Fig. 1). The Dpp-bian and Bipy ratio according to ^1H NMR spectrum is 1 : 3. The set of Dpp-bian signals corresponds to a symmetric ligand, which includes proton signals of the methine and methyl groups present in the isopropyl groups of the 2,6-$^i Pr_2C_6H_3$ substituents (CH: septet at δ 3.84 (4H) ppm; CH_3: doublets at δ 1.32 (12H) and 1.07 (12H) ppm). The aromatic protons appear in the δ 7.17–5.70 (12H) ppm range. The doublets at δ 8.69 (12H) and 7.67 (12H) ppm refer to neutral 4,4'-Bipy ligands. The presence of toluene and THF molecules in the crystal lattice of **II** is also confirmed by NMR spectroscopy data.

Thermogravimetric analysis was performed for complex **II** (Fig. 2). According to TGA data, there are three stages of thermal reactions until the compound is completely decomposed. The first stage (194–208°C, V_{max} at 198°C) involves the release of THF contained in the crystal cell. The second stage (208–306°C, V_{max} at 282°C) corresponds to the release of toluene, CO, and 4,4'-Bipy. Further heating (306–413°C, V_{max} at 352°C) leads to decomposition of the remaining complex to give amorphous products. Quantitative determination of the mass loss in each stage is difficult because they overlap.

According to X-ray diffraction data, crystalline compound **II** is a coordination polymer consisting of the sodium bipyridine cationic 3D framework $\{Na(4,4'\text{-Bipy})\}_n^+$, the cavities of which accommodate the heterobimetallic $\{(Dpp\text{-bian})GaCr(CO)_5\}^-$ anions and toluene and tetrahydrofuran solvation molecules (Fig. 3). The asymmetric part of the unit cell of **II** contains the $Na_2(4,4'\text{-Bipy})_6^{2+}$ dicationic moiety with the Na(1,2)N(5–16) atoms, two $\{(Dpp\text{-bian})GaCr(CO)_5\}^-$ anions, and one toluene and one THF molecule (Fig. 3b). The polymeric frame-

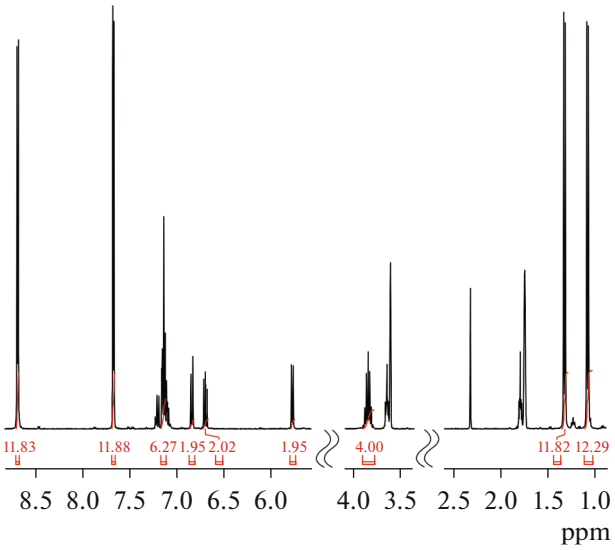

Fig. 1. ^{1}H NMR spectrum of compound **II** (400 MHz, C_4D_8O, 298 K).

work $\{Na(4,4'\text{-Bipy})\}_n^+$ has a primitive cubic cell pcu topology.

The structures of two symmetrically independent $\{(Dpp\text{-bian})GaCr(CO)_5\}^-$ anions are identical (Fig. 4). Analysis of the bond lengths in the metallacycle of **II** attests to the dianionic state of the Dpp-bian ligand: N(1)–C(1), N(3)–C(42) (1.38(4), 1.38(3) Å) and N(2)–C(2), N(4)–C(43) (1.36(3), 1.34(3) Å). The Ga–Cr bond lengths in **II** (2.393(5), 2.412(5) Å) are similar to that in the initial compound **I** (2.4219(3) Å) [22].

The solvent-accessible volume calculated by the Platon program [38] is 783 Å^3; this is equal to 11.3% of the volume of the unit cell, which contains one THF molecule and one toluene molecule (Fig. 5).

The use of Bpp ligand in the reaction with complex **I** leads to the formation of a three-dimensional coordination polymer $[(Dpp\text{-bian})GaCr(CO)_4Na(Et_2O)(Bpp)_{1.5}]_n$ (**III**) with a different structure (Scheme 2). The 3D framework of compound **III**, like that of **II**, is formed by means of sodium cations. The $\{(Dpp\text{-bian})GaCr(CO)_4\}^-$ anion remains bound to the sodium atom via one CO group, thus forming a contact ion pair. The reaction product was isolated as green crystals from the THF–diethyl ether solvent mixture (1 : 5) in 61% yield.

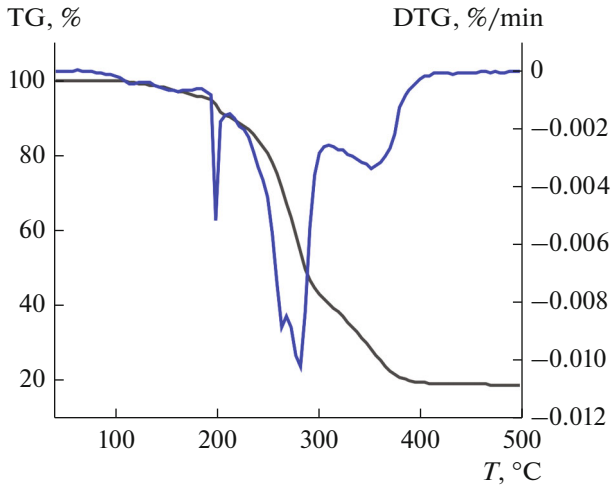

Fig. 2. Thermogravimetric analysis of **II**.

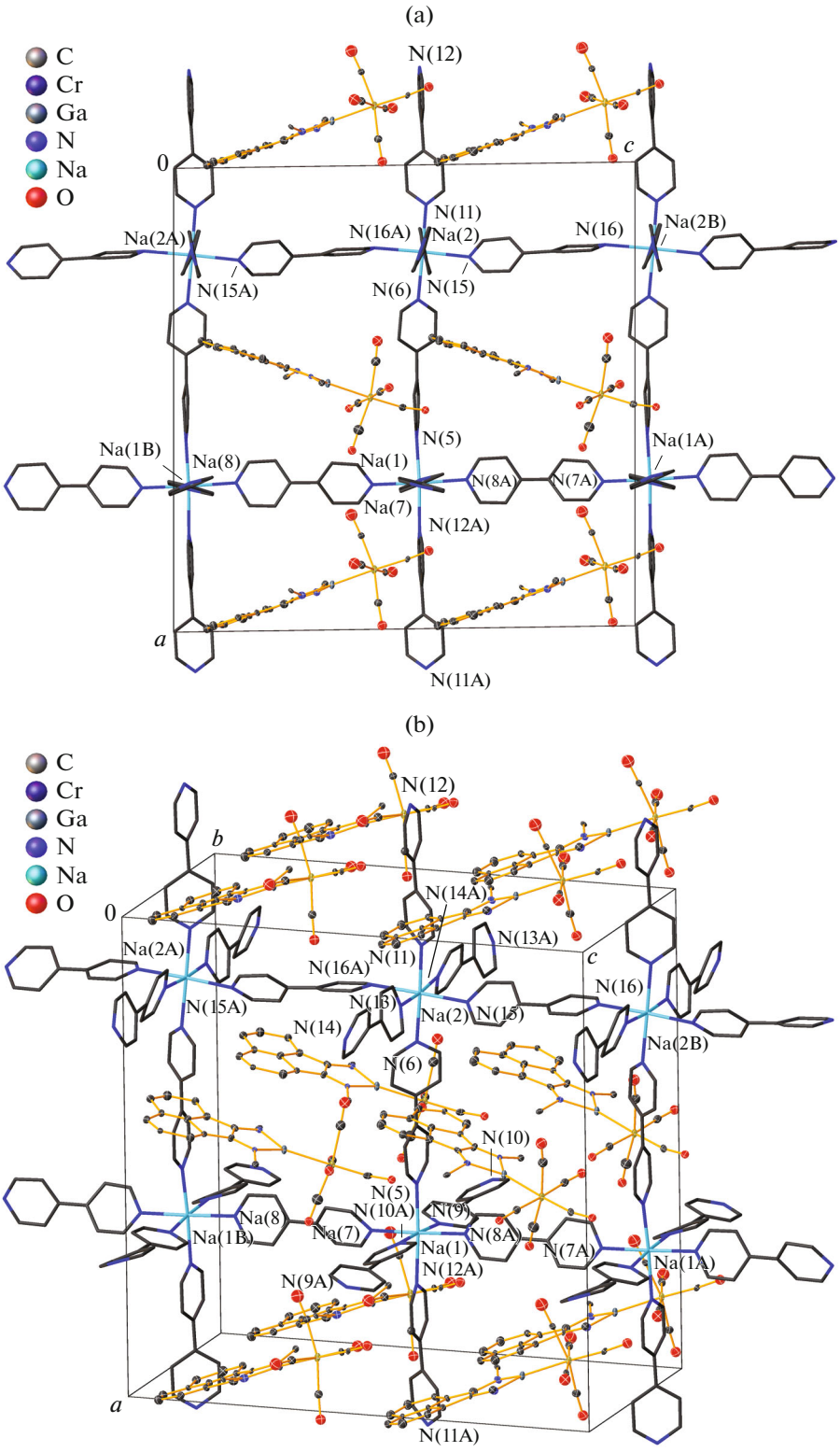

Fig. 3. Fragments of the crystal packing of **II**: (a) along the crystallographic *b* axis and (b) general view. The thermal ellipsoids of atoms of the anionic Ga–Cr complexes are given at 30% probability level. The hydrogen atoms, Ar substituents, and toluene and THF solvation molecules are not shown. Letter A indicates symmetrically equivalent atoms.

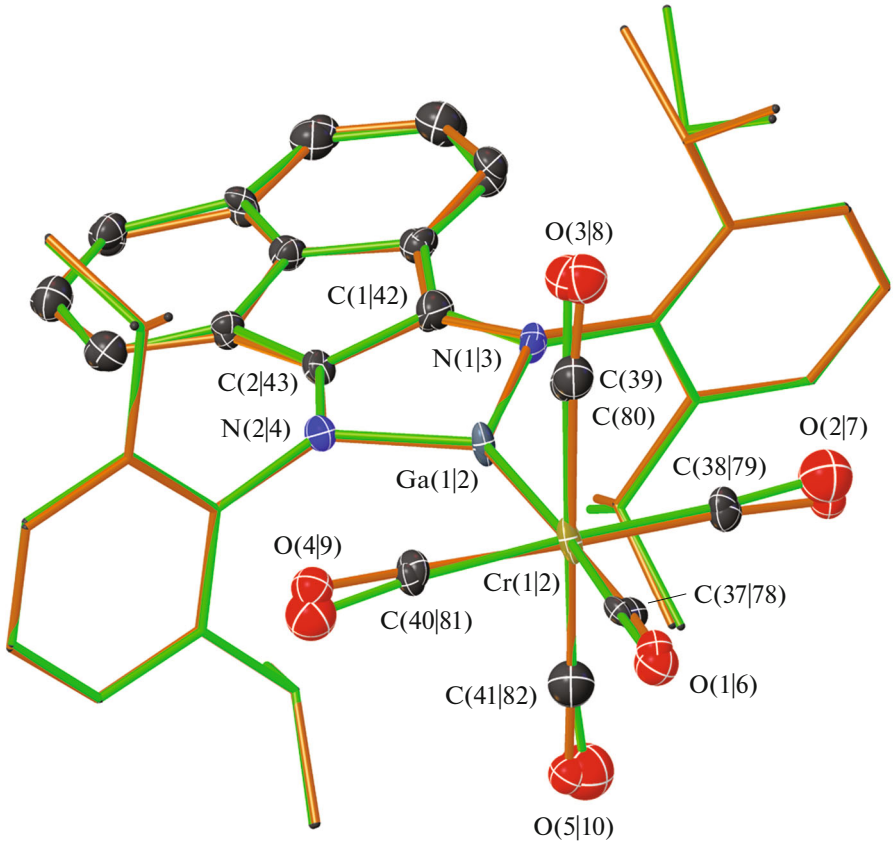

Fig. 4. Superposition of two independent molecules of the (Dpp-bian)$GaCr(CO)_5$ ionic complex in **II**. Thermal ellipsoids are given at 30% probability level. The hydrogen atoms are not shown. The symbol | separates the atom numbering for the first and second (Dpp-bian)$GaCr(CO)_5$ molecules (with green and brown bonds), respectively.

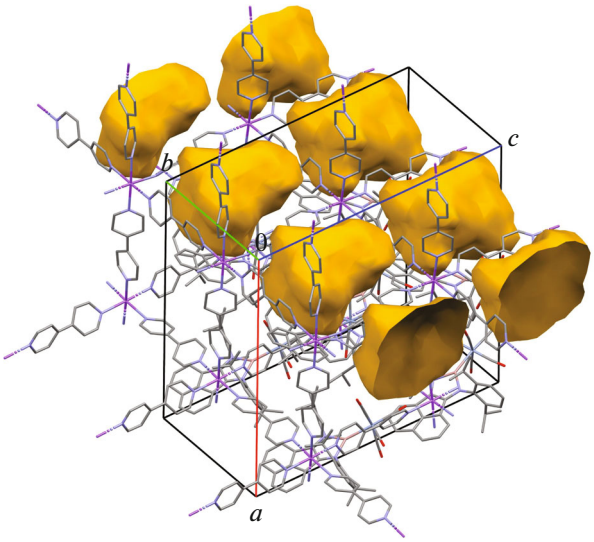

Fig. 5. Visualization of voids in the crystal of **II** using the Mercury program [39].

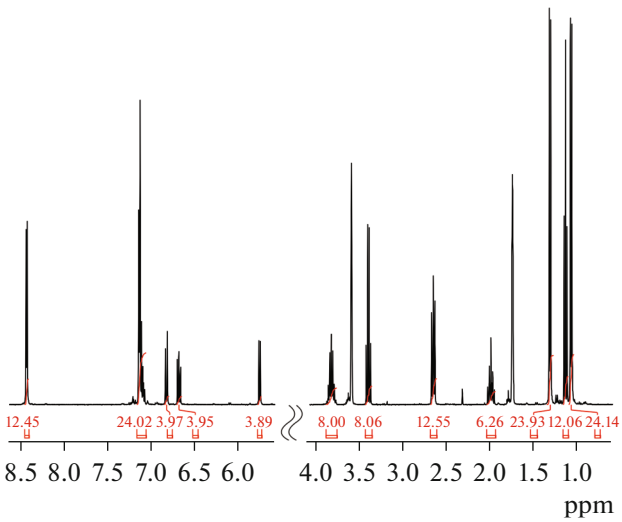

Fig. 6. ^1H NMR spectrum of compound **III** (400 MHz, C_4D_8O, 298 K).

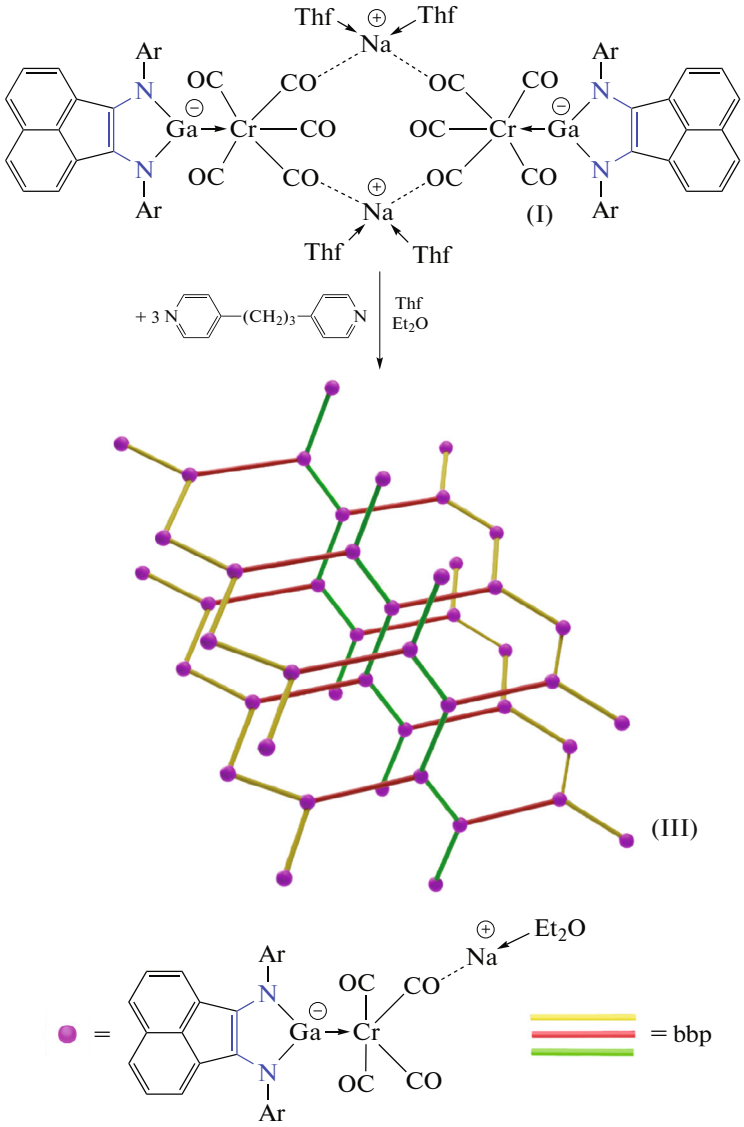

Scheme 2.

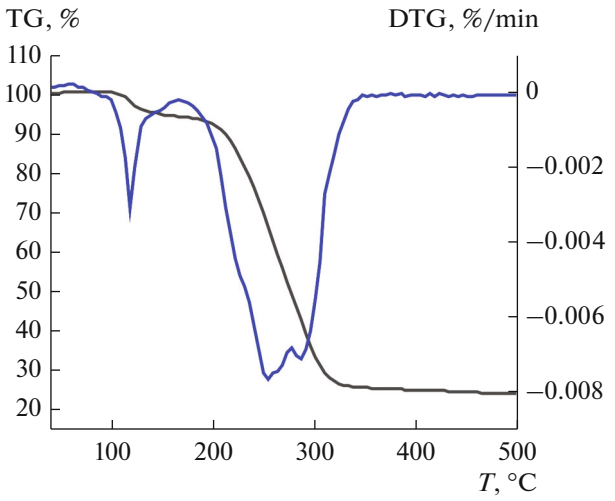

Fig. 7. Thermogravimetric analysis of **III**.

The IR spectrum of compound **III** exhibits intense absorption bands at 1897 and 2022 cm^{-1} corresponding to C–O stretching vibrations. The ^1H NMR spectrum of **III** (Fig. 6) shows proton signals for the methyl groups in the 2,6-$^i Pr_2C_6H_3$ substituents (doublets δ 1.08 (24H) and 1.31 (24H) ppm) and a septet for the methine protons (δ 3.83 (8H) ppm) of these substituents. The aromatic protons appear as four doublets in the δ 5.72–6.85 ppm range (12H) and a multiplet at δ 7.06–7.17 (24H) ppm comprising the protons (12H) of 1,3-bis(4-pyridyl)propane. The other signals of the Bpp ligand include a doublet at δ 8.44 (12H) (NC_5H_4), a triplet at δ 3.66 (12H) ppm, and a pentet at δ 1.99 (6H) ppm ($PyCH_2CH_2CH_2Py$). The signals for the diethyl ether are manifested at δ 3.40 (8H) and 1.33 (12H) ppm. The Dpp-bian and Bpp ratio, according to ^1H NMR data, is 2 : 3.

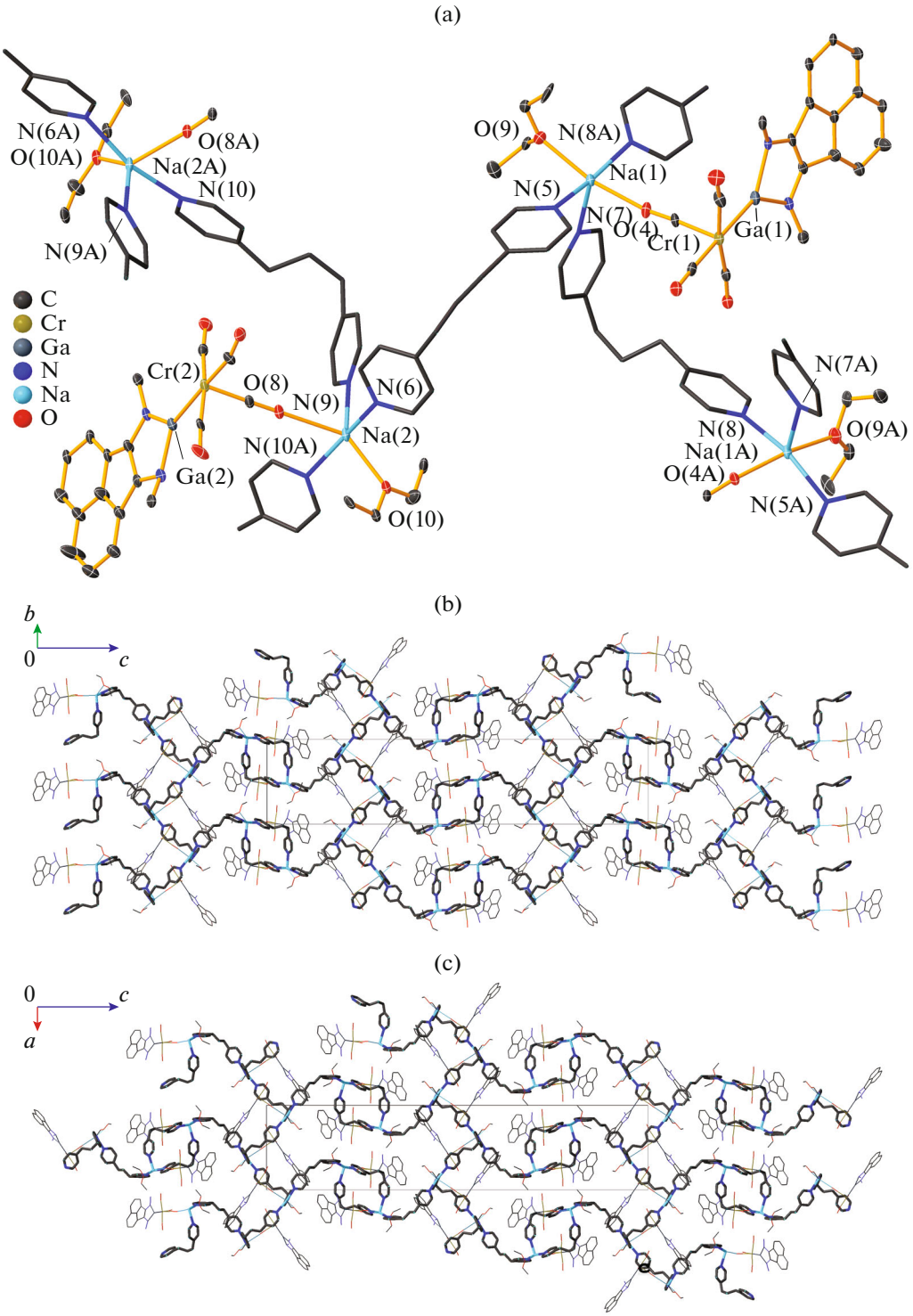

Fig. 8. (a) Asymmetric part of the 3D structure of **III** and (b, c) fragments of the crystal packing of **III** projected on the (b) *b*0*c* and (c) *a*0*c* planes. Letter A indicates symmetrically equivalent atoms.

The TGA study of product **III** (Fig. 7) revealed two stages of mass loss. The first stage (96–166°C, V_{max} at 119°C) is associated with the release of diethyl ether molecules. The mass loss at this stage is 6.5%. Further heating (166–348°C, V_{max} at 254°C) leads to degradation of the $\{(Dpp\text{-}bian)GaCr(CO)_4Na(Bpp)_{1.5}\}_n$ framework.

Unfortunately, only the relative positions of atoms in the crystals of complex **III** could be determined by X-ray diffraction analysis. According to X-ray diffraction data, compound **III** is a 3D MOCP (Fig. 8) in which the sodium atoms are linked together by bridging Bpp ligands and additionally coordinate {(Dpp-

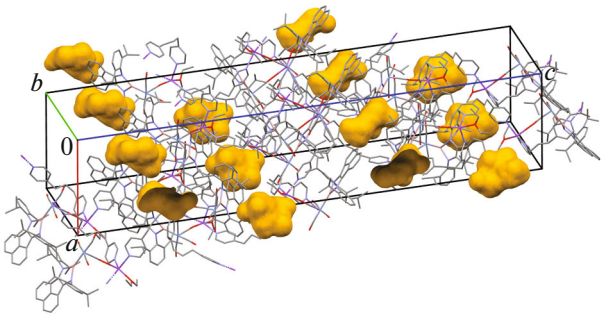

Fig. 9. Visualization of voids in the crystal of **III** using the Mercury program [39].

bian)GaCr(CO)$_4$}$^-$ anions and diethyl ether molecules. The monomer unit in **III** is the [{(Dpp-bian)GaCr(CO)$_4$Na(Et$_2$O)(Bpp)}(μ-Bpp){(Et$_2$O)(Bpp)Na(CO)$_4$CrGa(Dpp-bian)}] moiety (Fig. 3a). The trigonal bipyramidal environment of the sodium atom is formed by three nitrogen atoms from three different Bpp ligands and two oxygen atoms, one from the carbonyl CO ligand and one from diethyl ether. The structure of 3D coordination polymer **III** belongs to the ths topological type. The solvent-accessible volume calculated by the Platon program [38] is 542.1 Å^3, which makes 4.4% of the unit cell volume (Fig. 9).

Table 1. Crystallographic data and X-ray experiment and structure refinement details for **II**

Parameter	Value
Molecular formula	$C_{76.50}H_{72}N_8O_{5.50}NaCrGa$
M	1336.13
System	Monoclinic
Space group	*Pc*
Temperature, K	100(2)
Radiation wavelength, Å	0.71073
a, Å	23.8896(19)
b, Å	12.2089(7)
s, Å	23.806(2)
α, deg	90
β, deg	90.800(9)
γ, deg	90
V, Å^3	6942.7(9)
Z	4
ρ(calcd.), g/cm^3	1.278
μ, mm^{-1}	0.608
F(000)	2788
Crystal size, mm	0.56 × 0.36 × 0.11
Measurement range of θ, deg	1.873–25.027
Range indices	$-28 \le h \le 26$, $-14 \le k \le 13$, $-28 \le l \le 28$
Number of measured reflections	53304
Number of unique reflections (R_{int})	22708 (0.1211)
Number of reflections with $I > 2\sigma(I)$	14246
Absorption correction (max/min)	0.940/0.779
Data/constraints/parameters	22708/1339/1614
GOOF	1.050
R_1, wR_2 ($I > 2\sigma(I)$)	0.1176, 0.2461
R_1, wR_2 (for all reflections)	0.1750, 0.2878
Absolute structure parameter	0.358(17)
$\Delta\rho_{max}/\Delta\rho_{min}$, e Å^{-3}	2.947/–1.026

Table 2. Selected bond lengths (Å) and angles (deg) in compound **II**

Bond	*d*, Å	Angle	ω, deg
Ga(1)–N(1)	1.84(2)	Ga(2)–N(3)	1.88(2)
Ga(1)–N(2)	1.90(2)	Ga(2)–N(4)	1.91(2)
Ga(1)–Cr(1)	2.393(5)	Ga(2)–Cr(2)	2.412(5)
N(1)–C(1)	1.38(4)	N(3)–C(42)	1.38(3)
N(2)–C(2)	1.36(3)	N(4)–C(43)	1.34(3)
C(1)–C(2)	1.43(4)	C(42)–C(43)	1.35(4)
Cr(1)–C(C≡O)	1.77(3)–1.91(3)	Cr(2)–C(C≡O)	1.80(3)–1.95(4)
Na(1)–N(5)	2.39(3)	Na(2)–N(6)	2.48(3)
Na(1)–N(7)	2.41(2)	Na(2)–N(11)	2.44(2)
Na(1)–N(8A)	2.446(17)	Na(2)–N(13)	2.61(2)
Na(1)–N(9)	2.57(2)	Na(2)–N(14A)	2.56(3)
Na(1)–N(10A)	2.58(2)	Na(2)–N(15)	2.42(2)
Na(1)–N(12A)	2.51(3)	Na(2)–N(16A)	2.50(2)
Angle	ω, deg	Angle	ω, deg
N(1)Ga(1)N(2)	88.1(10)	N(3)Ga(2)N(4)	86.1(13)
C(37)Cr(1)Ga(1)	174.5(8)	C(78)Cr(2)Ga(2)	177.4(10)
C(38)Cr(1)C(40)	175.1(13)	C(79)Cr(2)C(81)	175.7(12)
C(39)Cr(1)C(41)	165.6(13)	C(80)Cr(2)C(82)	168.7(15)
C(37)Cr(1)C(38)	97.7(12)	C(78)Cr(2)C(79)	93.1(12)
C(37)Cr(1)C(39)	97.9(13)	C(78)Cr(2)C(80)	94.0(14)
C(37)Cr(1)C(40)	84.6(11)	C(78)Cr(2)C(81)	91.2(12)
C(37)Cr(1)C(41)	95.6(12)	C(78)Cr(2)C(82)	96.3(15)
Ga(1)Cr(1)C(38)	87.7(9)	Ga(2)Cr(2)C(79)	89.1(9)
Ga(1)Cr(1)C(39)	81.3(10)	Ga(2)Cr(2)C(80)	84.7(10)
Ga(1)Cr(1)C(40)	90.0(8)	Ga(2)Cr(2)C(81)	86.6(8)
Ga(1)Cr(1)C(41)	85.7(8)	Ga(2)Cr(2)C(82)	85.2(12)
C(38)Cr(1)C(39)	87.1(14)	C(79)Cr(2)C(80)	87.7(15)
C(39)Cr(1)C(40)	96.9(13)	C(80)Cr(2)C(81)	92.4(14)
C(40)Cr(1)C(41)	89.4(13)	C(81)Cr(2)(82)	91.9(16)
C(41)Cr(1)C(38)	86.1(13)	C(82)Cr(2)C(79)	87.2(16)
N(5)Na(1)N(12A)	177.0(7)	N(6)Na(2)N(11)	178.0(9)
N(7)Na(1)N(8A)	178.4(14)	N(13)Na(2)N(14A)	175.7(11)
N(9)Na(1)N(10A)	176.0(7)	N(15)Na(2)N(16A)	177.7(10)
N(5)Na(1)N(7)	88.9(12)	N(6)Na(2)N(13)	93.0(9)
N(5)Na(1)N(8A)	89.5(9)	N(6)Na(2)N(14A)	91.0(9)
N(5)Na(1)N(9)	87.8(10)	N(6)Na(2)N(15)	88.8(9)
N(5)Na(1)N(10A)	93.1(10)	N(6)Na(2)N(16A)	89.4(9)
N(12A)Na(1)N(7)	88.1(12)	N(11)Na(2)N(13)	85.2(8)
N(12A)Na(1)N(8A)	93.5(9)	N(11)Na(2)N(14A)	90.8(9)
N(12A)Na(1)N(9)	92.5(10)	N(11)Na(2)N(15)	92.2(9)
N(12A)Na(1)N(10A)	86.8(9)	N(11)Na(2)N(16A)	89.5(8)
N(7)Na(1)N(9)	91.5(10)	N(13)Na(2)N(16A)	89.9(8)
N(8A)Na(1)N(9)	88.4(9)	N(16A)Na(2)N(14A)	88.6(9)
N(7)Na(1)N(10A)	92.4(10)	N(14A)Na(2)N(15)	89.9(10)
N(8A)Na(1)N(10A)	87.8(9)	N(15)Na(2)N(13)	91.7(9)

Thus, in this study, we obtained two 3D MOCPs of different topologies. Both compounds considered in this paper contain gallaimidazole [(Dpp-bian)Ga:] moieties, in which the metal atoms occur in low oxidation states. Despite the enormous number of MOCPs synthesized to date, 2D and 3D coordination polymers containing low-valent nodes in their lattice are not numerous and are represented by only transition metal derivatives [40]. This provides the conclusion that derivatives **II** and **III** are unique examples of 3D MOCPs containing main group metals in low oxidation state.

ACKNOWLEDGMENTS

This study was performed using research equipment of the Center for Collective Use "Analytical Center of the Razuvaev Institute of Organometallic Chemistry, Russian Academy of Sciences," supported by the grant "Provision of the Development of Material and Technical Infrastructure of Centers for Collective Use of Research Equipment" (RF–2296.61321X0017, agreement number 075-15-2021-670).

FUNDING

This study was supported by the Russian Science Foundation (project no. 19-13-00336-П).

CONFLICT OF INTEREST

The authors of this work declare that they have no conflicts of interest.

REFERENCES

1. Hadlington, T.J., Driess, M., and Jones, C., *Chem. Soc. Rev.*, 2018, vol. 47, p. 4176.
2. Chu, T. and Nikonov, G.I., *Chem. Rev.*, 2018, vol. 118, p. 3608.
3. Zhong, M., Sinhababu, S., and Roesky, H.W., *Dalton Trans.*, 2020, vol. 49, p. 1351.
4. Hardman, N.J., Eichler, B.E., and Power, Ph.P., *Chem. Commun.*, 2000, no. 20, p. 1991.
5. Jin, G., Jones, C., Junk, P.C., et al., *New J. Chem.*, 2008, vol. 32, p. 835.
6. Overgaard, J., Jones, C., Dange, D., and Platts, J.A., *Inorg. Chem.*, 2011, vol. 50, p. 8418.
7. Jones, C., Junk, P.C., Platts, J.A., and Stasch, A., *J. Am. Chem. Soc.*, 2006, vol. 128, no. 7, p. 2206.
8. Schmidt, E.S., Jockisch, A., and Schmidbaur, H., *J. Am. Chem. Soc.*, 1999, vol. 121, no. 41, p. 9758.
9. Schmidt, E.S., Schier, A., and Schmidbaur, H., *Dalton Trans.*, 2001, no. 5, p. 505.
10. Baker, R.J., Farley, R.D., Jones, C., et al., *Dalton Trans.*, 2002, no. 20, p. 3844.
11. Dange, D., Choong, S.L., Schenk, Ch., et al., *Dalton Trans.*, 2012, vol. 41, p. 9304.
12. Morris, L.J., Rajeshkumar, T., Maron, L., and Okuda, J., *Chem.-Eur. J.*, 2022, vol. 28, no. 56, p. e202201480.
13. Seifert, A., Scheid, D., Linti, G., and Zessin, T., *Chem.-Eur. J.*, 2009, vol. 15, no. 44, p. 12114.
14. Jones, C., Mills, D.P., and Rose, R.P., *J. Organomet. Chem.*, 2006, vol. 691, no. 13, p. 3060.
15. Kassymbek, A., Britten, J.F., Spasyuk, D., et al., *Inorg. Chem.*, 2019, vol. 58, no. 13, p. 8665.
16. Kassymbek, A., Vyboishchikov, S.F., Gabidullin, B.M., et al., *Angew. Chem., Int. Ed. Engl.*, 2019, vol. 58, p. 18102.
17. Baker, R.J., Jones, C., and Platts, J.A., *Dalton Trans.*, 2003, no. 19, p. 3673.
18. Baker, R.J., Jones, C., and Platts, J.A., *J. Am. Chem. Soc.*, 2003, vol. 125, no. 35, p. 10534.
19. Aldridge, S., Baker, R.J., Coombs, N.D., et al., *Dalton Trans.*, 2006, no. 27, p. 3313.
20. Jones, C., Mills, D.P., Rose, R.P., et al., *J. Organomet. Chem.*, 2010, vol. 695, no. 22, p. 2410.
21. Fedushkin, I.L., Sokolov, V.G., Piskunov, A.V., et al., *Chem. Commun.*, 2014, vol. 50, p. 10108.
22. Fedushkin, I.L., Sokolov, V.G., Makarov, V.M., et al., *Russ. Chem. Bull.*, 2016, vol. 65, no. 6, p. 1495.
23. Sokolov, V.G., Skatova, A.A., Piskunov, A.V., et al., *Russ. Chem. Bull.*, 2020, vol. 69, no. 8, p. 1537.
24. Dodonov, V.A., Sokolov, V.G., Baranov, E.V., et al., *Inorg. Chem.*, 2022, vol. 61, no. 38, p. 14962.
25. Zhang, R., Wang, Y., Zhao, Y., et al., *Dalton Trans.*, 2021, vol. 50, no. 39, p. 13634.
26. Koptseva, T.S., Sokolov, V.G., Ketkov, S.Yu., et al., *Chem.-Eur. J.*, 2021, vol. 27, no. 18, p. 5745.
27. Sokolov, V.G., Koptseva, T.S., Rumyantcev, R.V., et al., *Organometallics*, 2020, vol. 39, no. 1, p. 66.
28. Koptseva, T.S., Bazyakina, N.L., Baranov, E.V., and Fedushkin, I.L., *Mendeleev Commun.*, 2023, vol. 33, p. 167.
29. Koptseva, T.S., Moskalev, M.V., Baranov, E.V., and Fedushkin, I.L., *Organometallics*, 2023, vol. 42, p. 965.
30. Koptseva, T.S., Bazyakina, N.L., Moskalev, M.V., et al., *Eur. J. Inorg. Chem.*, 2021, no. 7, p. 675.
31. Koptseva, T.S., Bazyakina, N.L., Rumyantcev, R.V., and Fedushkin, I.L., *Mendeleev Commun.*, 2022, vol. 32, p. 780.
32. *Data Collection, Reduction and Correction Program. CrysAlisPro 1.171.42.76a - Software Package*, Rigaku OD, 2022.
33. Sheldrick, G.M., *Acta Crystallogr., Sect. A: Cryst. Adv.*, 2015, vol. 71, p. 3.
34. Sheldrick G.M., *SHELXTL. Version 6.14. Structure Determination Software Suite*, Madison: Bruker AXS, 2003.
35. Sheldrick, G.M., *Acta Crystallogr., Sect. C: Struct. Chem.*, 2015, vol. 71, p. 3.
36. *SCALE3 ABSPACK: Empirical Absorption Correction, CrysAlisPro 1.171.42.76a - Software Package*, Rigaku OD, 2022.
37. Blatov, V.A., Shevchenko, A.P., and Proserpio, D.M., *Cryst. Growth Des.*, 2014, vol. 14, p. 3576.
38. Spek, A.L., *Acta Cryst.*, 2009, vol. 65, p. 148.
39. Macrae, C.F., Sovago, I., Cottrell, S.J., et al., *J. Appl. Crystallogr.*, 2020, vol. 53, p. 226.
40. Sikma, R.E., Balto, K.P., Figueroa, J.S., and Cohen, S.M., *Angew. Chem., Int. Ed. Engl.*, 2022, vol. 61, p. e202206353.

Translated by Z. Svitanko